

Riverine phosphorus gain and loss across the conterminous United States

Yiming Wang¹, Xuesong Zhang², Kaiguang Zhao¹, Robert D. Sabo³, Yuxin Miao⁴, Christopher M. Clark³

1. Ohio Agricultural Research and Development Center, School of Environment and Natural Resources, The Ohio State University, Wooster, OH 44691, USA

2. USDA-ARS Hydrology and Remote Sensing Laboratory, Beltsville, MD, 20705-2350, USA

3. United States Environmental Protection Agency, Office of Research and Development, Center for Public Health and Environmental Assessment, Health and Environmental Effects Assessment Division, Washington, DC, 20460, USA.

4. Precision Agriculture Center, Department of Soil, Water and Climate, University of Minnesota, St. Paul, MN 55108, USA

Correspondence to: Yiming Wang (wang.20415@osu.edu); Xuesong Zhang (Xuesong.Zhang@usda.gov)

Abstract. Excess riverine phosphorus represents a preeminent catalyst for water quality degradation. Spatial mapping and characterization of the net gain and loss of riverine phosphorus help discern the critical source areas. Here, we developed a dataset encompassing phosphate (PO_4^{3-}) and total phosphorus (TP) gain and loss across catchments in the conterminous United States (CONUS). We compiled 51,394 PO_4^{3-} and 285,675 TP concentration measurements and estimated PO_4^{3-} and TP loads at 963 and 2,317 stations, respectively. Next, we leveraged the upstream-downstream topology information from the National Hydrography Dataset Plus (NHDPlus) catchment map at the Hydrologic Unit Catalogue-12 (HUC12) level to derive the net gain and loss of riverine phosphorus across catchments in the CONUS. Such maps can be used to estimate potential contributions of point and non-point sources to riverine phosphorus pollution at refined spatial scales, identify different major factors controlling local riverine P gain and loss compared to P loads, and evaluate watershed model's fidelity for representing riverine P cycling. The resultant dataset is provided in Excel (.xlsx) format, accessible at Figshare (<https://doi.org/10.6084/m9.figshare.28509317>, Wang et al., 2025). Leveraging the HUC12 information for spatialization, the new datasets aim to address the existing gap in regional characterization of riverine phosphorus and support effective management practices across the CONUS.

Deleted: data points

Deleted: (<https://doi.org/10.6084/m9.figshare.28509317>,

Deleted:).

Formatted: Font color: Black

29 **1 Introduction**

30 Eutrophication [in inland waters and estuaries](#) is a widespread water quality challenge across the globe, with significant
31 economic cost (e.g., \$1 billion in Europe and \$2.2 billion annually in the United States (U.S.)) (Wurtsbaugh et al., 2019).

32 Excess phosphorus (P) is a primary contributor to eutrophication in streams and rivers, especially in intensive agricultural
33 regions (Brownlie et al., 2022; Royer et al., 2006). Riverine export of P is also a major contributor to oxygen-depleted dead
34 zones in coastal waters, causing damage to underwater life (Diaz and Rosenberg, 2008). There is an urgent need for global
35 actions to reduce P pollution for the environment and human health (UNEP, 2025).

36 Nonpoint or diffuse sources, particularly nutrients applied to agroecosystems, are often recognized as the primary source of
37 water pollution (Carpenter et al., 1998). P surplus in agricultural soils due to [unused](#) fertilization and manure application can
38 be transported to water bodies through surface runoff and groundwater pathways, and cause persistent water pollution
39 (Stackpoole et al., 2019). The [diffuse nature of nonpoint source pollution](#) poses challenges for directly identifying and
40 regulating critical source areas. Existing riverine P pollution databases mainly focus on certain agricultural areas (Ringeval et
41 al., 2024). Given the considerable spatial variation in P inputs to rivers (Arheimer and Lidén, 2000; Stackpoole et al., 2019;
42 Zhang et al., 2017), there is a lack of large-scale riverine P datasets at sufficient spatial scales across the conterminous United
43 States (CONUS) to quantify and analyze riverine P gain and loss. Such datasets, in conjunction with other observed and
44 modelled P data (e.g., point source discharge) help identify regions with high non-point source P inputs, thereby supporting
45 more effective targeting of measures for P pollution control. In addition, the datasets can also be used to assess fidelity of
46 distributed watershed models and understand key factors influencing local riverine P cycling.

47 In this study, we aim to develop new datasets for spatial characterization of riverine P gain and loss across the CONUS, to
48 help identify critical source areas and improve prioritization and implementation of nutrient management activities. The
49 subsequent sections of this paper include the method used to generate spatial riverine P gain and loss (Section 2), results
50 detailing the P dataset (Section 3), discussion of influencing factors and potential uncertainties (Section 4), codes and data
51 availability (Section 5), and conclusions (Section 6).

52

53 **2 Materials and Methods**

54 **2.1 Overview**

55 To estimate riverine P gain and loss data across the CONUS, we compiled streamflow and P concentration data (i.e., unfiltered
56 phosphate (PO_4^{3-}) [from 963 monitoring stations](#) and total phosphorus (TP) [from 2,317 stations](#), and calculated P loads at [these](#)
57 stations using the Load Estimator (LOADEST) program (Runkel et al., 2004) (Fig. 1). Next, we estimated P gain and loss
58 across the catchments measured by one downstream station and its immediate upstream stations using the upstream-
59 downstream connectivity information contained in the National Hydrography Dataset Plus (NHDPlus) catchments

Deleted:).

Deleted: 2006a).

Deleted:).

Deleted:).

Deleted:).

Deleted: excessive

Deleted:).

Deleted:).

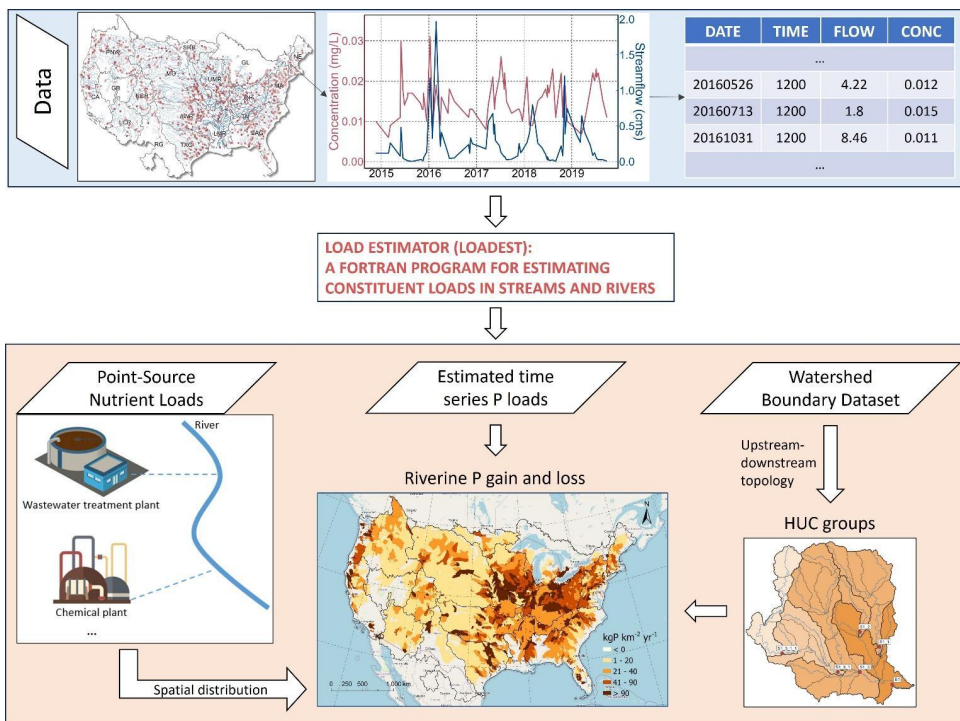
Deleted:).

Deleted: at over 1,000 hydrological

Deleted: in the CONUS

Deleted: those

72 (https://nhdplus.com/NHDPlus/NHDPlusV2_data.php), resulting in 547 and 1,225 unique Hydrologic Unit Catalogue (HUC)
 73 groups for PO_4^{3-} and TP, respectively. Each HUC group has a unique pair of downstream and upstream stations that allows us
 74 to calculate the gain and loss of riverine P (as illustrated in Fig. S1 in the Supplemental Information). Note that headwater
 75 HUC groups only have one downstream station without upstream stations draining to them. Due to differences in data
 76 availability, the riverine PO_4^{3-} and TP gain and loss data cover 52,020 and 65,735 Hydrologic Unit Catalogue-12 (HUC12)
 77 catchments, respectively. Then we estimated potential contribution to P pollution from nonpoint sources by subtracting
 78 upstream P inputs and point source P inputs from the riverine P gain and loss in each catchment. Finally, we used land cover
 79 and climate data to evaluate major controls of riverine P gain and loss.



80
 81 **Figure 1: Overview of the generation of TP and PO_4^{3-} gain and loss data across the CONUS A more detailed description and higher**
 82 **resolution figure about HUC group generation can be found in Text S2 and Fig. S1.**

83 2.2 Study area

84 The CONUS (i.e., the lower 48 states of the U.S.) is located in North America from 46° 20' to 98° 34' W longitude and from
85 39° 49' to 41° 43' N latitude, covering an area of 8,080,464.3 km² with a north-to-south distance of approximately 2,660 km.
86 The terrain features higher elevations in the west and flatter areas in the east. Based on the Watershed Boundary Dataset (WBD;
87 <https://water.usgs.gov/GIS/huc.html>), the CONUS includes 18 major watersheds, encompassing several large rivers such as
88 the Mississippi and Colorado Rivers.

89 2.3 Data compilation

90 We compiled 51,394 PO₄³⁻ (USGS parameter code 00650) concentration data from 963 stations (spanning from 1952 to 2022)
91 and 285,675 TP (USGS parameter code 00665) observations from 2,317 stations (spanning from 1958 to 2023) across the
92 CONUS from the Water Quality Portal (Read et al., 2017). To ensure consistency with streamflow records, only records from
93 the U.S. Geological Survey (USGS) National Water Information System (NWIS) data source were used in this study. For each
94 P observation, we identified co-located monitoring stations (Wang, Zhang, Zhao, et al., 2024) and downloaded and processed
95 daily streamflow data from the USGS NWIS. Only stations with both phosphorus concentration observations and
96 corresponding daily streamflow records were retained. We calculated an average P concentration where there were multiple P
97 concentration observations on the same day. Before calculating the P load at a station with the LOADEST model, we excluded
98 stations with less than 12 measurements. Thus, we finally selected 547 stations for PO₄³⁻ and 1,225 stations for TP. For TP,
99 the "Point-Source Nutrient Loads to Streams of the Conterminous United States" dataset provides estimated annual total point-
100 source inputs during 2012 at the HUC12 level (Skinner and Maupin, 2019). This allowed us to aggregate the total TP input to
101 rivers for the catchments used to calculate riverine TP gain and loss. Note that the point source dataset does not contain PO₄³⁻.

102 Land cover and climatic controls of riverine P gain and loss were also assessed. Land cover data were derived from the National
103 Land Cover Database (NLCD; <https://doi.org/10.5066/P94UXNTS>), which provided long-term average information on
104 various land cover types: barren land, crops, forest, hay, herbs, impervious surfaces, scrub, water, herbaceous wetlands, and
105 woody wetlands (Homer et al., 2012). Climate data were sourced from the PRISM dataset
106 (<https://www.prism.oregonstate.edu/>), including annual average temperature and total precipitation (Page et al., 2021). Using
107 upstream-downstream topology information, we calculated the total area of each land cover type from the headwater to the
108 current catchment at the HUC12 scale, representing their cumulative impact. For climate data, the local climate within each
109 HUC12 was used. The P surplus was accessed from the National Inventory of Phosphorus (NIP), which provides major inputs
110 and outputs of reactive P at the HUC8 scale across the CONUS (Sabo et al., 2021).
111 To ensure consistency across datasets with different spatial resolutions, all analyses were anchored at the HUC12 group scale.
112 Point-source inputs, originally reported at the HUC12 level, were aggregated to HUC12 groups to match the gain-loss estimates.
113 For datasets available at coarser scales (e.g., HUC8 for NIP inputs and HUC4 for agricultural inputs), gain and loss were
114 upscaled using area-weighted averaging. No downscaling was applied.

Deleted: to 46° 20'

Deleted: hydrological

Deleted: hydrological

Deleted:).

Deleted: hydrological

Deleted: U.S. Geological Survey (USGS) National Water Information System...

Deleted: hydrological

Deleted: data points

Deleted:).

Deleted:).

Deleted:).

Deleted:).

2.4 Riverine P gain and loss across catchments in the CONUS

Riverine P gain and loss was estimated by calculating the difference between P loads at a downstream monitoring station and the sum of P loads from its neighbouring upstream stations. For multiple USGS stations located in the same HUC12 catchment, we kept only one station on the mainstem of the river that is closest to the outlet of the HUC12 catchment, by comparing the drainage area of the gaging station and the HUC12 catchment in which it is located. For headwaters, since there are no upstream gages, the P load was used as the net riverine gain. The upstream-downstream topology relationship between the monitoring stations was derived from the HUC12 catchments from the watershed boundary dataset (WBD; <https://water.usgs.gov/GIS/huc.html>). Such a method has been outlined and tested by Qiu et al. (2023) (Text S2). As explained above, we identified 547 and 1,225 unique HUC groups for PO₄³⁻ and TP, respectively. Note that each HUC group includes multiple HUC12 polygons and these HUC12 catchments share the same gain and loss data.

For each HUC group, the balance of riverine P can be expressed as follows:

$$P \text{ load at downstream outlet} = (P \text{ loads from upstream inputs}) + (P \text{ from point sources}) - (P \text{ from non-point sources}) - (P \text{ from non-point sources}) \quad (1)$$

Because in-stream removal terms cannot be directly constrained and may vary across systems (e.g., about 12% globally (Maavara et al., 2015), we assume the values of these two terms to be negligible for the purpose of deriving a simplified, first-order estimate for nonpoint source inputs. Thus, riverine removal is not explicitly estimated in this study, and the calculated P gain and loss represent the net difference between downstream and upstream loads. Conceptually, this net difference reflects the combined effects of watershed P inputs (from both point and nonpoint sources) and in-stream processes (e.g., retention, transformation, and remobilization) occurring along the flow path, rather than a direct measure of any single process such as in-stream removal. Under this assumption, Eq. (1) reduces to:

$$(P \text{ from nonpoint sources}) = P \text{ gain and loss} - (P \text{ from point sources}) \quad (2)$$

where $P \text{ gain and loss} = (P \text{ load at downstream outlet}) - (P \text{ loads from upstream inputs})$.

Accordingly, negative values of P gain and loss indicate net decreases in load along the flow path, which may reflect a combination of retention, transformation, or other processes, rather than being interpreted solely as riverine removal. This formulation neglects in-stream P removal, and therefore $(P \text{ from nonpoint sources}) = P \text{ gain and loss} - (P \text{ from point sources})$ is a lower-end estimate of the nonpoint source contribution to riverine P for each HUC group. Since only TP from point sources is available, we derived nonpoint-source TP loads but not for PO₄³⁻.

2.5 Evaluation of estimated riverine load

We evaluated the consistency of the PO₄³⁻ and TP loads against another independent dataset derived with the Weighted Regressions on Time, Discharge, and Season (WRTDS) model (Hirsch et al., 2010; Zhang and Hirsch, 2019). First, we compared multi-year average TP loads from 151 monitoring stations. We also evaluated the estimated unfiltered PO₄³⁻ loads,

Deleted: hydrological

Deleted: hydrological

Deleted: <object>Rearranging the above equation leads to:
 $(P \text{ from nonpoint sources}) = P \text{ gain and loss} - (P \text{ from point sources}) + (P \text{ from nonpoint sources}) - (P \text{ from nonpoint sources})$

Formatted: Font: Times New Roman

Deleted: Given that rivers often remove a small portion of P load (e.g., 12%) (Maavara et al., 2015), we assumed that

Deleted: .

Deleted: hydrological

171 which assess the mass of reactive P susceptible to being released in the water column under various redox conditions.
172 Furthermore, the reliability of the upstream-downstream connectivity information is important for deriving the drainage area
173 of HUC groups that are controlled by pairs of upstream and downstream stations. Here we used a quality-checked and corrected
174 NHDPlus HUC12 catchment map (Wang, Zhang, & Zhao, 2024) that has been verified for reliably deriving the drainage area
175 of each USGS station as compared to the USGS GAGES-II reported values (Falcone and Survey, 2011). These efforts helped
176 ensure the quality of the riverine P gain and loss data developed in this study. In addition, we evaluated long-term trends in
177 riverine P loads using the Sen's slope estimator in combination with the Mann-Kendall test (Hamed and Rao, 1998). To ensure
178 robust trend detection, only monitoring stations with more than 30 years of load estimates were included. This resulted in 405
179 TP stations and 53 PO₄³⁻ stations used for trend analysis. The Sen's slope and corresponding p-values are provided in the
180 dataset.

Deleted: hydrological

Deleted: hydrologic

Deleted:).

181 2.6 Analysis of environmental controls

182 Recent studies reveal that shifts in land use, agricultural practices, and climatic conditions have introduced a pervasive increase
183 in soluble P concentrations across many different watersheds (Houser and Richardson, 2010; Singh et al., 2023). To assess the
184 spatial factors influencing riverine P gain and loss, we employed random forest modelling to evaluate the relative importance
185 of multiple environmental variables (Breiman, 2001). These factors were categorized into three groups: climatic factors, land
186 cover types, and additional influences such as cumulative agricultural inputs and upstream loads. Given that the NIP dataset is
187 only available at the HUC8 scale and some HUC groups are larger than the HUC8 catchment areas, we calculated the
188 cumulative agricultural inputs at the HUC4 scale. In more detail, we used the ranger package, optimizing the model structure
189 with the caret package in R. Key tuning parameters included the number of variables to use in each split (mtry), the number of
190 trees (n_trees) and the minimum size of data points before splitting a tree (min_n). The tuning process was performed by doing
191 a grid search for mtry (2-6) and min_n (10-20), then a second search was performed to find the optimal n_trees parameter
192 (500-3000). To minimize random effects, the model was run 10 times, and we calculated the average importance value and
193 harmonic mean p-value (Wilson, 2019).

Deleted:).

Deleted:).

Deleted:).

194 3 Results

195 3.1 Riverine phosphorus data

196 We created two datasets, "Riverine PO₄³⁻" and "Riverine TP," that encapsulate estimated multi-year average riverine gain and
197 loss and loads, as well as point source and nonpoint source contributions for each HUC group for PO₄³⁻ and TP, respectively
198 (Table 1). Complementing this information, the datasets encompass the location (i.e., longitude and latitude) of the outlet of
199 the HUC group, the area of the HUC group, the count of observations used to calculate P loads, and commencement and
200 termination years of observed data, to facilitate user-defined subsetting of the datasets. Additional information regarding the

207 regression model is also included, such as the form of the regression model selected by LOADEST and the associated
 208 coefficient of determination (r^2) values.

209 Across the board, the average r^2 values for the best-fit model (Table S1) across all sites are 0.76 for PO_4^{3-} loads and 0.83 for
 210 TP loads. Generally, in the load regression, the r^2 values for TP estimation outperformed those for PO_4^{3-} estimation, particularly
 211 in the Mid-Atlantic region (Fig. S2). It is noteworthy, however, that certain monitoring stations exhibited low r^2 values due to
 212 the limited availability of paired P concentration with streamflow data for regression.

213

214 **Table 1. Data records in the "Riverine PO_4^{3-} " and "Riverine TP" datasets.**

| Field name | Description |
|-------------------------------|---|
| Station ID | U.S. Geological Survey designated ID; Note that this ID is also used to denote a unique HUC group |
| Lat | Latitude of the <u>monitoring</u> station at the outlet of a HUC group |
| Long | Longitude of the <u>monitoring</u> station at the outlet of a HUC group |
| Area | Area of the HUC group |
| Load | The amount of PO_4^{3-} or TP loads at the outlet station of a HUC group (kgP yr^{-1}) |
| P gain and loss | The difference between P loads at the outlet of a HUC group and all its immediate upstream stations ($\text{kgP km}^{-2} \text{yr}^{-1}$) |
| NonPts TP contribution* | Nonpoint-source contribution to riverine phosphorus from a HUC group ($\text{kgP km}^{-2} \text{yr}^{-1}$) |
| Pts TP load | Point-source TP loads (kg yr^{-1}) from a HUC group |
| obsNum | The number of phosphorus concentration data with paired streamflow data |
| startYr | The starting year of the observed data |
| endYr | The ending year of the observed data |
| modelID | The ID of regression model used for load estimation |
| r2 | R-Squared (%) for the selected LOADEST regression model used to estimate the P load |
| <u>Sen's slope</u> | <u>Sen's slope of riverine P loads, representing the long-term rate of change in loads at monitoring stations (kg yr^{-2}).</u> |
| <u>p-value</u> | <u>The p-value of long-term trends</u> |
| <u>Areal-normalized slope</u> | <u>Areal-normalized Sen's slope of riverine P loads, representing the long-term rate of change in areal P export ($\text{kg km}^{-2} \text{yr}^{-2}$).</u> |

215 Note: * only for TP as only point source TP inputs are available.

216

217 Our TP load estimates are highly consistent with the WRTDS model with high r^2 and low root mean square error (RMSE)
 218 (Fig. 2). The minor disparities observed between these two datasets are likely attributable to variations in temporal coverage.

Deleted: hydrologic

Formatted Table

Deleted: hydrologic

Deleted: hydrologic

Deleted: hydrologic

Deleted: .

and different regression equations. For PO_4^{3-} , we found that only 11 stations with WRTDS estimates matched the stations used here, and all 11 stations are located in small watersheds. Therefore, we leveraged filtered PO_4^{3-} loads estimated by WRTDS to assess if the LOADEST estimated unfiltered PO_4^{3-} loads. Unfiltered PO_4^{3-} measures both the dissolved PO_4^{3-} as well as PO_4^{3-} compounds bound to suspended sediments and organic materials, and thus will have higher load compared to filtered PO_4^{3-} measurements (Fig. S3). Nonetheless, the high correlation indicates our estimates of unfiltered PO_4^{3-} are reasonable.

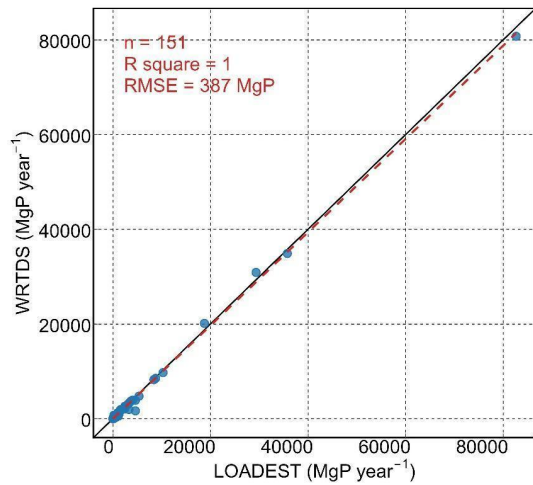


Figure 2: Comparison of riverine TP loads between our estimates and previous WRTDS estimated values at 151 monitoring stations. Note that the riverine TP loads vary greatly at different locations and over time, with most sites being below 10,000 MgP year⁻¹.

Spatial patterns of PO_4^{3-} and TP loads from each HUC group across the CONUS are shown in Fig. 3. Additionally, the location of the station at the outlet of each HUC group and the loads of streams in which it is located are shown in Fig. S4. The datasets encompass 547 stations/HUC groups for PO_4^{3-} and 1,225 stations/HUC groups for TP, covering 4,894,464 and 6,118,360 km² PO_4^{3-} and TP, respectively. At the HUC2 scale, the derived gain and loss estimates cover 21% to 99.9% of basin area for TP and 7% to 96.5% for PO_4^{3-} , with 72% and 44% of HUC2 basins exceeding 50% coverage, respectively (Fig. S5 and Table S2). The difference in spatial coverage is mainly due to the abundance of TP compared to PO_4^{3-} . Stations with high P loads are predominantly situated in the Midwest or proximate to megacities, with a general pattern of higher P loads observed in the eastern U.S. PO_4^{3-} loads range from 111 to 31,671,885 kgP yr⁻¹ and TP loads range from 235 to 336,223,136 kgP yr⁻¹. Median loads are 76,202 and 108,305 kgP yr⁻¹ and average loads are 436,311 and 1,012,363 kgP yr⁻¹, for PO_4^{3-} and TP, respectively. We further examined temporal trends in riverine P loads at stations with long-term records (>30 years). A substantial fraction of stations exhibited statistically significant trends, with 46% of TP stations and 64% of PO_4^{3-} stations showing significant

Deleted: S2

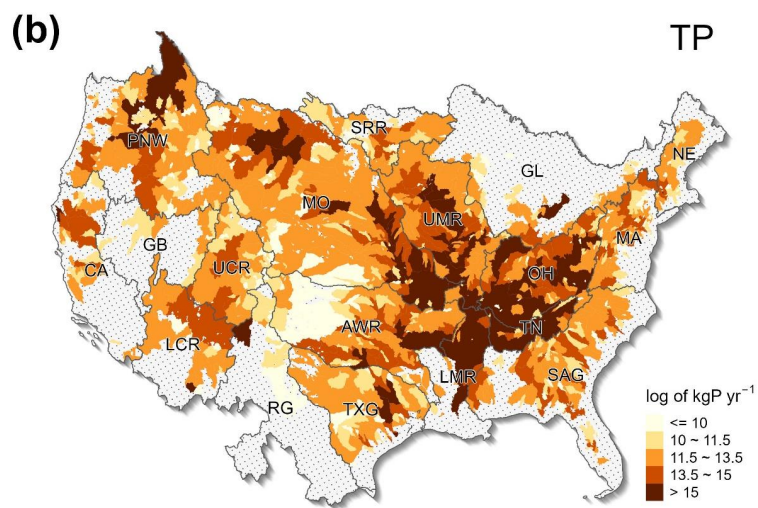
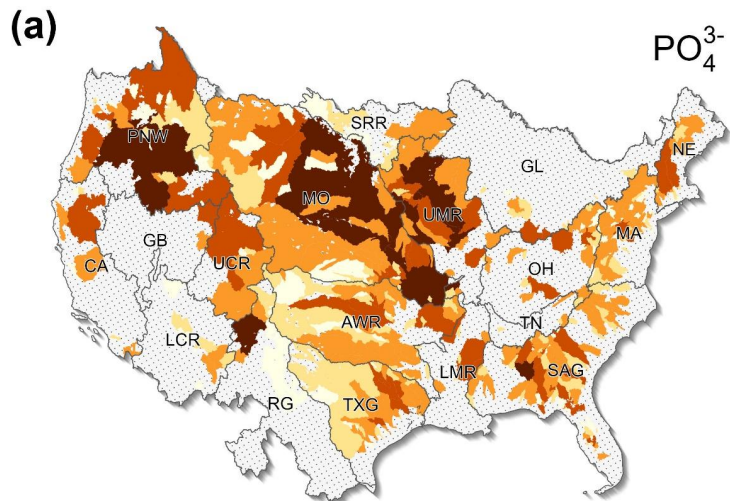
Deleted: hydrological

Deleted: hydrologic

Deleted: S3

Deleted: hydrologic

249 changes. Decreasing trends were more prevalent, accounting for 72% and 58% of TP and PO₄³⁻ stations, respectively. Stations
250 with increasing TP trends were primarily located in the Mississippi River Basin (Fig. S6), suggesting regional differences in
251 nutrient dynamics.



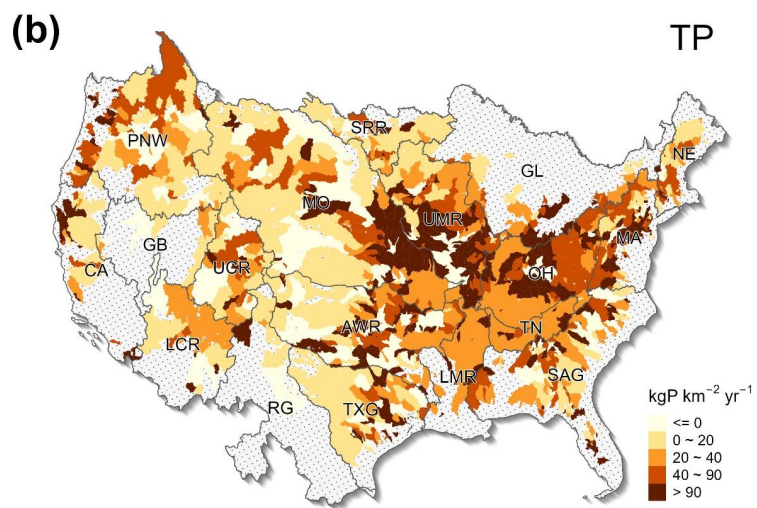
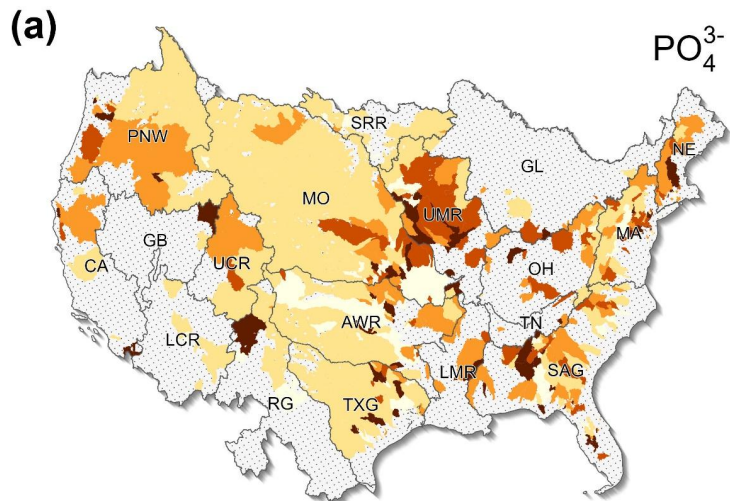
253 **Figure 3: Riverine (a) PO₄³⁻ and (b) TP loads from HUC groups across the CONUS. The boundary lines show the Hydrologic Unit**
254 **Catalogue 2-digit (HUC2) watersheds. Grey areas indicate regions with no data. For visualization purposes, the logarithm was used**
255 **here.**

256

257 The spatial distribution of riverine P gain and loss is shown in Fig. 4. Both PO₄³⁻ and TP gain and loss exhibit similar spatial
258 patterns over the CONUS, with most areas exhibiting riverine P gains. The area-weighted average PO₄³⁻ gain stands at 25.39
259 kgP km⁻² yr⁻¹, and the TP gain is 33.68 kgP km⁻² yr⁻¹. Median PO₄³⁻ and TP gains are lower than averages, standing at 16.75
260 kgP km⁻² yr⁻¹ and 33.57 kgP km⁻² yr⁻¹, respectively. At the HUC group scale, the highest area-weighted PO₄³⁻ gain was
261 identified in the Upper Mississippi Region (UMR), amounting to about 113.96 kgP km⁻² yr⁻¹. The highest TP gain reached
262 186.55 kgP km⁻² yr⁻¹ in the Tennessee Region (TN). Notably, widespread regions in the Midwest exhibit heightened P gains,
263 (Fig. S7), particularly in terms of PO₄³⁻, suggesting a discernible impact of human activities (e.g., agricultural fertilization). At
264 the HUC2 level, the lowest area-weighted PO₄³⁻ gain (1.72 kgP km⁻² yr⁻¹) was found in the Rio Grande Region (RG), and the
265 lowest TP gain (0.62 kgP km⁻² yr⁻¹) was found in the Upper Colorado Region (UCR). Refined examination at the HUC group
266 level showed that, over the CONUS, 392,778 km² and 1,468,973 km² areas exhibited riverine PO₄³⁻ and TP losses, respectively.

267

Deleted: ,



270 **Figure 4: The spatial distribution of the gain and loss in riverine (a) PO_4^{3-} and (b) TP over the CONUS. The boundary lines show**
271 **the Hydrologic Unit Catalogue 2-digit (HUC2) watersheds. Grey areas indicate regions with no data.**

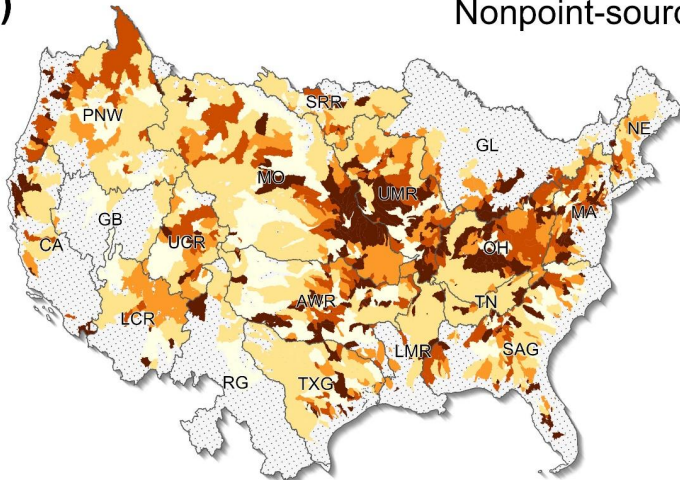
272

273 **3.2 Point and nonpoint source contributions**

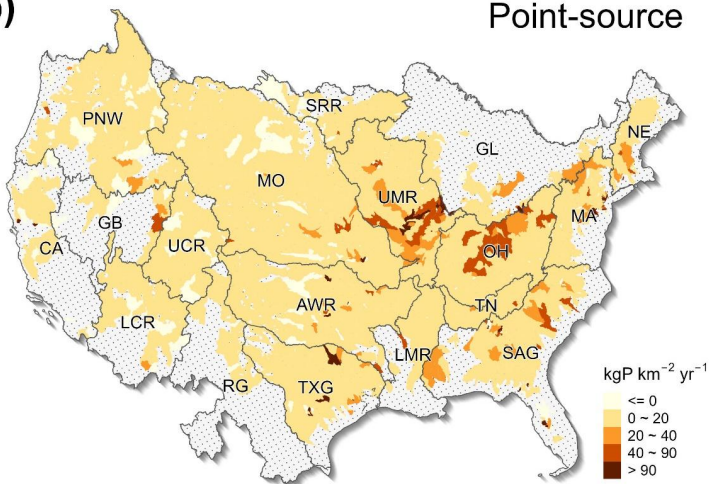
274 We also mapped the spatial point source and nonpoint source inputs of TP, as shown in Fig. 5. The nonpoint source
275 contributions are estimated based on Equation (2), which provides a lower-end estimate given that the riverine removal of
276 point and nonpoint source P as shown in Equation (2) was not considered. Point and nonpoint source contributions to riverine
277 TP pollution exhibited large differences in both the magnitude and spatial distribution. Over the CONUS, the area-averaged
278 point source input of TP is $5.44 \text{ kgP km}^{-2} \text{ yr}^{-1}$. By subtracting point source inputs from the calculated TP gain and loss, we
279 obtained an area-averaged nonpoint source TP contribution of $28.24 \text{ kgP km}^{-2} \text{ yr}^{-1}$. Regions characterized by high TP gain with
280 minimal point source pollution were observed in the Midwest. Notably, in most of the agriculturally intensive Missouri and
281 Tennessee-Ohio river basins, total nonpoint source discharge significantly surpassed point source contributions (Fig. S8). Upon
282 the exclusion of point source contributions (Fig. 5b), there is a substantial change, with the areas with riverine TP losses
283 expanding to $1,603,258 \text{ km}^2$, most of them in the Missouri and Arkansas-White-Red River Basins. In general, most watersheds
284 with negative nonpoint sources are concentrated in the western U.S. This does not mean that the nonpoint source P inputs are
285 negative, but indicates that riverine processes likely removed a large fraction of point and nonpoint source P.

Deleted: .

(a) Nonpoint-source



(b) Point-source



288 **Figure 5: The spatial distribution of (a) nonpoint source and (b) point source contributions to riverine P pollution over the CONUS.**
289 **The boundary lines show the Hydrologic Unit Catalogue 2-digit (HUC2) watersheds. Grey areas indicate regions with no data.**

290

291 3.3 Factors influencing TP

292 We employed a random forest model to assess the influence of climate, land use, human activities, and catchment
293 characteristics on riverine TP gain and loss and TP loads (Fig. 6). Note that the calculated P loads represent the outcome of
294 the entire upstream catchment processes, while the riverine P gain and loss data represent both upstream catchment processes
295 (e.g., P inputs from upstream) and local catchment properties (e.g., climate and land use in a HUC group). Such differences
296 lead to the use of different sets of influencing factors (Fig. 6). The land use, climate and point source factors were calculated
297 for the entire upstream area draining to a monitoring station for TP load analysis. In contrast, those factors were averaged over
298 a HUC group for riverine gain and loss analysis. Additionally, for the analysis of riverine P gain and loss data, we included
299 upstream P inputs. Analysis results indicate that upstream input is the sole statistically significant factor affecting TP gain and
300 loss, with climate and land cover showing no notable impact. Conversely, TP loads are predominantly influenced by climatic
301 factors, alongside significant contributions from point source discharges and urban land use.

Deleted: hydrological

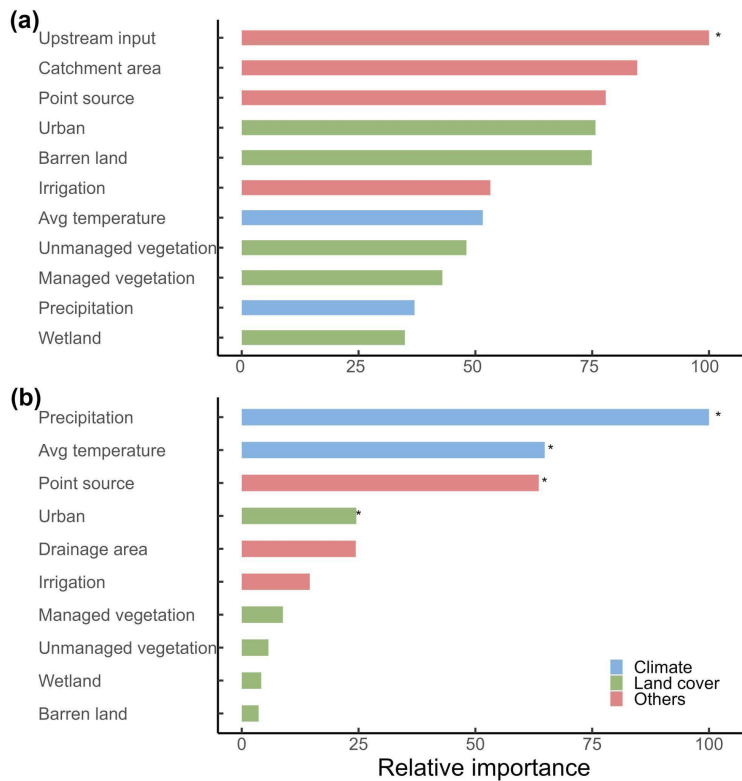


Figure 6: The importance of factors influencing (a) TP gain and loss and (b) TP loads. Asterisks indicate significance at a level of 0.05.

4 Discussion

4.1 Important contributions from nonpoint sources to riverine P pollution

The estimated area-averaged nonpoint source TP contribution ($28.24 \text{ kgP km}^{-2} \text{ yr}^{-1}$) represents a reduction of 16.2% from the calculated TP gain and loss that includes contributions from both point and nonpoint sources ($33.68 \text{ kgP km}^{-2} \text{ yr}^{-1}$). Given that the TP inputs from point and nonpoint sources are often subject to riverine removal (Withers and Jarvie, 2008), the estimated nonpoint source TP based on Equation (1) should be augmented by the amount of total TP inputs (including both nonpoint and point source) removed through riverine processes. Therefore, the calculated nonpoint source inputs of TP represent an

Deleted: (Maavara et al., 2015),

314 underestimate of the contributions from nonpoint sources. If we assume a 12% removal rate for TP inputs (Maavara et al.,
315 2015), then the nonpoint source inputs of TP would increase from 28.24 kgP km⁻² yr⁻¹ to 32.28 kgP km⁻² yr⁻¹. Collectively, the
316 results show that the nonpoint sources likely contribute more than 84% of riverine TP pollution.

Deleted:),

317 4.2 Implications for analysing environmental controls of riverine P

318 Climatic factors were key drivers of TP loads at the outlet of a watershed, which in general aligns with findings from previous
319 studies (Sabo et al., 2023) and underscores the role of climate in nutrient transport dynamics. Our environmental control
320 analysis using the gain and loss data showed that upstream inputs are leading control of local riverine gain and loss (Fig. 6a),
321 in addition to local inputs of P from point and nonpoint sources and local riverine processes, such as in-stream retention through
322 mechanisms such as P absorption by periphyton via photosynthesis and hydrological processes like reduced streamflow and
323 sedimentation (Dodds, 2003; Withers and Jarvie, 2008). Notably, although accumulated agricultural P inputs (i.e., livestock
324 waste and agricultural fertilizer) positively influenced TP gain and loss (Fig. S9), they were not included in this analysis due
325 to mismatch of spatial scales. In general, using TP loads and riverine P gain and loss can lead to pronounced differences in the
326 analysis of importance of environmental controls. Although climate conditions (i.e., precipitation and temperature) are the
327 major controls of TP loads, which represent the integration of the entire watershed conditions, while riverine P gain and loss
328 indicate that the amount of upstream P inputs entering a local catchment is an important factor influencing the riverine
329 processing of P.

Deleted:).

Deleted: S4

330 Both the differences and the analysis using TP loads and riverine gain and loss data revealed the importance of urban land and
331 agricultural management. For example, both analyses show that irrigation can influence riverine TP, indicating that improving
332 irrigation efficiency and technology holds potential to reduce TP inputs from cropland fertilization (Xia et al., 2020). Though
333 we didn't assess factors influencing PO₄³⁻ due to the lack of point source PO₄³⁻ data, TP hotspots are expected to occur further
334 downstream than PO₄³⁻ hotspots (Fig. 3). This is probably because rivers typically can retain (e.g., periphyton assimilation,
335 adsorption onto suspended or bed sediment) a considerable proportion of incoming soluble-reactive P (e.g., PO₄³⁻) within the
336 upper network, whereas particulate P continue to transport to downstream (Jarvie et al., 2012; Robertson and Saad, 2019;
337 Royer et al., 2006). Overall, the intricate interplay between climate and land use factors underscores the complex nature of P
338 dynamics in riverine systems. These newly developed riverine gain and loss datasets help improve understanding of local
339 controls of riverine P dynamics and identify hotspots of changes in riverine P.

Deleted:).

Deleted: 2006b).

340 4.3 Limitations and contribution

341 While the newly developed datasets leverage upstream-downstream topology information at the HUC12 level to help increase
342 the spatial resolution of riverine P gain and loss data, it is essential to acknowledge limitations relevant to understanding and
343 quantifying P cycles and identifying sources of P inputs. First, the accuracy of load estimation via LOADEST is contingent
344 upon the availability of paired P concentration data from monitoring stations. Stations with limited observations may introduce

Deleted: hydrological

351 higher uncertainties in load estimations. The robustness of our datasets is partially reflected in the number of observations
352 available. The average and median numbers of PO₄³⁻ observations per site is 54 and 29, respectively; for TP, the average and
353 median numbers of observations per site is 134 and 90, respectively. In addition, the average center year of TP observations is
354 1992, with a median of 1991, while for PO₄³⁻, the overall observation time is relatively early, with an average of 1981 and a
355 median of 1980. The use of AIC to choose the most parsimonious regression model (average r² of 0.76 and 0.83 for PO₄³⁻ and
356 TP, respectively) helped reduce uncertainties in load estimates.

357 Additionally, we calculated the P loads by averaging over different time periods with available data for each monitoring station.
358 The mismatch between observational periods of upstream and downstream stations could introduce uncertainties, given that
359 the available data cover various time periods for different stations. For example, streamflow discharge, which is important for
360 calculating nutrient loads, can vary from year to year. Here, we assumed that multi-year average estimates of P loads are
361 representative of the long-term pattern at a monitoring station. This may not hold for some upstream and downstream stations
362 covering time periods that do not overlap with each other. Therefore, we provided the number and period of observations and
363 model performance information in the datasets, which can help users to refine the calculation of riverine P gain and loss by
364 further screening the P loads data at the monitoring stations. Note that available stations with observed P concentration and
365 streamflow data are relatively sparse in the western vs. eastern U.S., particularly for PO₄³⁻. This led to large gaps in the spatial
366 coverage of the datasets (Fig. 4). Increasing the number of stations with P observations holds the potential to enhance the
367 accuracy of riverine P estimates in the future.

368 It is also worth noting that the calculated contribution of TP from nonpoint sources represents a conservative estimate, given
369 the unknown rate of TP removal from point and nonpoint sources. Although previous studies showed that TP removal rates
370 were generally small, they could vary substantially across regions, as evidenced by the areas with riverine P loss (Fig. 4). It is
371 reasonable to assume that the estimated TP contribution from nonpoint sources is greater than 84% over the CONUS; however,
372 the local TP contribution from nonpoint sources could be much lower, particularly in regions with high point source inputs.
373 Also, the removal rates of P from point and nonpoint sources are likely different due to differences in the quality of P inputs
374 (e.g., biodegradability and adsorption and desorption to sediments) and flow pathways (Wang et al., 2025a). Therefore, caution
375 should be taken when interpreting the local contribution to P pollution from nonpoint sources.

376 Despite these challenges, our datasets make a unique contribution to the quantification and analysis of riverine P load, gain
377 and loss, and sources across the CONUS. They can support the evaluation and diagnosis of large-scale dynamic watershed
378 models, the examination of environmental controls on riverine P loads, and the estimation of contributions to P gain and loss.
379 For instance, models such as SPARROW could incorporate the spatial patterns of riverine P gain and loss to better constrain
380 nutrient sources and in-stream processing across river networks. The insights derived from our datasets contribute to a more
381 comprehensive understanding of P dynamics under long-term and multi-decadal conditions, providing a foundation for
382 improved water quality management on local, regional, and national scales.

Deleted: hydrological

Deleted: hydrological

Deleted: hydrological

Deleted: hydrological

Deleted: hydrological

Deleted: hydrologic

Deleted: hydrological

Deleted: 2025).

391 **5 Code and data availability**

392 All codes for validating and visualizing PO₄³⁻ and TP gain and loss from the load estimations were run in R version 4.3.1 and
393 are archived at https://github.com/ymwang4924/gain-loss_P. The datasets presented in the paper are available at
394 <https://doi.org/10.6084/m9.figshare.28509317> (Wang et al., 2025b).

Deleted: 2025).

Formatted: Font color: Black

395 **6 Conclusions**

396 In this study, we estimated riverine loads of PO₄³⁻ and TP and derived their gain and loss across the CONUS, leveraging the
397 upstream-downstream hydrological connectivity information contained in the NHDPlus catchment map. On average, rivers
398 across the CONUS gain TP at a rate of 33.68 kgP km⁻² yr⁻¹, with notable hotspots in the Midwest. Due to the limitations of
399 data availability, the precision of estimated P gain and loss data could be influenced by the number and periods of observations
400 available at upstream and downstream stations. We provided additional information regarding the number of observations
401 available, temporal coverage of data, the regression model used, and the model's statistical performance, so that users can
402 further subset the datasets to meet certain specific criteria.

403 The riverine P gain and loss datasets allow the estimation of riverine P removal or accrual at a refined spatial resolution to
404 better reflect the impacts of local controls. In contrast, riverine P loads at monitoring stations embody the integrated processes
405 from the entire area upstream of a specific station. Also, by combining point source inputs with the riverine P gain and loss
406 datasets, we derived conservative estimates of the long-term average contribution of nonpoint sources to riverine TP (28.24
407 kgP km⁻² yr⁻¹). The control factor analysis with a random forest model demonstrated that upstream inputs had the greatest
408 influence on the local riverine P gain and loss, while climatic factors dominated riverine P loads at monitoring stations. This
409 suggests that nutrient management practices that prioritize enhancing irrigation efficiency and integrating strategies such as
410 targeted fertilizer application and wetland restoration may more effectively capture and reduce phosphorus mobilization from
411 agricultural lands. The newly developed riverine P datasets in this study extend utility to diverse applications, encompassing,
412 but not limited to, the evaluation of watershed models, identification of critical source areas, and optimization of agricultural
413 management strategies. Future studies may concentrate on filling gaps in the spatial and temporal coverage of the datasets
414 (particularly for PO₄³⁻).

Deleted: hydrological

Deleted: hydrological

415 **Author contributions**

416 **Y.W.:** Conceptualization, methodology, investigation, formal analysis, data curation, visualization, and writing—original
417 draft. **X.Z.:** Conceptualization, methodology, investigation, writing—original draft, writing—review and editing, supervision,
418 project administration, and funding acquisition. **K.Z.:** methodology, investigation, writing—review and editing. **R.D.S.:**
419 investigation, writing—review and editing. **Y.M.:** visualization, writing—review and editing. **C.M.C.:** writing—review and
420 editing.

424 **Competing interests**

425 At least one of the (co-)authors is a member of the editorial board of *Earth System Science Data*.

426 **Disclaimer**

427 The views expressed are those of the authors, and do not necessarily represent the views or policies of the U.S. Environmental
428 Protection Agency or any other Federal agency. Any use of trade, firm, or product names is for descriptive purposes only and
429 does not imply endorsement by the U.S. Government.

430 **Financial support**

431 This research is in part supported by the U.S. Department of Agriculture – Agricultural Research Service and the National
432 Aeronautics and Space Administration (NASA 22-CMS22-0027). The mention of trade names or commercial products in this
433 publication is solely for the purpose of providing specific information and does not imply recommendation or endorsement by
434 the funding agencies.

435 **Acknowledgement**

436 We thank Sarah Stackpoole, Qian Zhang, and Kate Schofield for constructive comments and editorial suggestions on earlier
437 versions of the manuscript.

438 **References**

439 Arheimer, B. and Lidén, R.: Nitrogen and phosphorus concentrations from agricultural catchments—influence of spatial and
440 temporal variables, *J Hydrol (Amst)*, 227, 140–159, [https://doi.org/10.1016/S0022-1694\(99\)00177-8](https://doi.org/10.1016/S0022-1694(99)00177-8), 2000.

441 Breiman, L.: Random Forests, *Mach. Learn.*, 45, 5–32, <https://doi.org/10.1023/A:1010933404324>, 2001.

442 Brownlie, W. J., Sutton, M. A., Heal, K. V., Reay, D. S., and Spears, B.: Our phosphorus future: towards global phosphorus
443 sustainability, 2022.

444 Carpenter, S. R., Caraco, N. F., Correll, D. L., Howarth, R. W., Sharpley, A. N., and Smith, V. ~~H.:~~ **NONPOINT POLLUTION**
445 **OF SURFACE WATERS WITH PHOSPHORUS AND NITROGEN**, *Ecological Applications*, 8, 559–568,
446 <https://doi.org/10.1890/1051-0761>, 1998.

447 Diaz, R. J. and Rosenberg, R.: Spreading Dead Zones and Consequences for Marine Ecosystems, *Science* (1979), 321, 926–
448 929, <https://doi.org/10.1126/science.1156401>, 2008.

Formatted: Font: 10 pt

Deleted: ,

Deleted: H.: Nonpoint pollution of surface waters with phosphorus and nitrogen

452 Dodds, W. K.: THE ROLE OF PERIPHYTON IN PHOSPHORUS RETENTION IN SHALLOW FRESHWATER AQUATIC
453 SYSTEMS, *J Phycol*, 39, 840–849, <https://doi.org/10.1046/j.1529-8817.2003.02081.x>, 2003.

454 Falcone, J. A. and Survey, U. S. G.: GAGES-II: Geospatial Attributes of Gages for Evaluating Streamflow, Reston, VA,
455 <https://doi.org/10.3133/70046617>, 2011.

456 Hamed, K. H. and Rao, A. R.: A modified Mann-Kendall trend test for autocorrelated data, *J. Hydrol. (Amst.)*, 204, 182–196,
457 1998.

458 Hirsch, R. M., Moyer, D. L., and Archfield, S. A.: Weighted Regressions on Time, Discharge, and Season (WRTDS), with an
459 Application to Chesapeake Bay River Inputs ¹, *JAWRA Journal of the American Water Resources Association*, 46, 857–880,
460 <https://doi.org/10.1111/j.1752-1688.2010.00482.x>, 2010.

461 Homer, C. G., Fry, J. A., and Barnes, C. A.: The national land cover database, 2012.

462 Houser, J. N. and Richardson, W. B.: Nitrogen and phosphorus in the Upper Mississippi River: Transport, processing, and
463 effects on the river ecosystem, *Hydrobiologia*, 640, 71–88, <https://doi.org/10.1007/s10750-009-0067-4> TABLES/2, 2010.

464 Jarvie, H. P., Sharpley, A. N., Scott, J. T., Haggard, B. E., Bowes, M. J., and Massey, L. B.: Within-River Phosphorus Retention:
465 Accounting for a Missing Piece in the Watershed Phosphorus Puzzle, *Environ. Sci. Technol.*, 46, 13284–13292,
466 <https://doi.org/10.1021/es303562y>, 2012.

467 Maavara, T., Parsons, C. T., Ridenour, C., Stojanovic, S., Dürr, H. H., Powley, H. R., and Van Cappellen, P.: Global
468 phosphorus retention by river damming, *Proceedings of the National Academy of Sciences*, 112, 15603–15608,
469 <https://doi.org/10.1073/pnas.1511797112>, 2015.

470 Page, M. J., Moher, D., Bossuyt, P. M., Boutron, I., Hoffmann, T. C., Mulrow, C. D., Shamseer, L., Tetzlaff, J. M., Akl, E. A.,
471 Brennan, S. E., Chou, R., Glanville, J., Grimshaw, J. M., Hróbjartsson, A., Lalu, M. M., Li, T., Loder, E. W., Mayo-Wilson,
472 E., McDonald, S., McGuinness, L. A., Stewart, L. A., Thomas, J., Tricco, A. C., Welch, V. A., Whiting, P., and McKenzie, J.
473 E.: PRISMA 2020 explanation and elaboration: updated guidance and exemplars for reporting systematic reviews, *BMJ*, 372,
474 <https://doi.org/10.1136/BMJ.N160>, 2021.

475 Qiu, H., Zhang, X., Yang, A., Wickland, K. P., Stets, E. G., and Chen, M.: Watershed carbon yield derived from gauge
476 observations and river network connectivity in the United States, *Scientific Data* 2023 10:1, 10, 1–13,
477 <https://doi.org/10.1038/s41597-023-02162-7>, 2023.

478 Read, E. K., Carr, L., De Cicco, L., Dugan, H. A., Hanson, P. C., Hart, J. A., Kreft, J., Read, J. S., and Winslow, L. A.: Water
479 quality data for national-scale aquatic research: The Water Quality Portal, *Water Resour Res*, 53, 1735–1745,
480 <https://doi.org/10.1002/2016WR019993>, 2017.

481 Ringeval, B., Demay, J., Goll, D. S., He, X., Wang, Y. P., Hou, E., Matej, S., Erb, K. H., Wang, R., Augusto, L., Lun, F.,
482 Nesme, T., Borrelli, P., Helfenstein, J., McDowell, R. W., Pletnyakov, P., and Pellerin, S.: A global dataset on phosphorus in
483 agricultural soils, *Scientific Data* 2024 11:1, 11, 1–34, <https://doi.org/10.1038/s41597-023-02751-6>, 2024.

484 Robertson, D. M. and Saad, D. A.: Spatially referenced models of streamflow and nitrogen, phosphorus, and suspended-
485 sediment loads in streams of the midwestern United States, <https://doi.org/10.3133/sir20195114>, 2019.

Deleted: K.: The role of periphyton in phosphorus retention in shallow freshwater aquatic systems

Formatted: Superscript

Deleted: s10750

Deleted: ,

490 Royer, T. V., David, M. B., and Gentry, L. E.: Timing of Riverine Export of Nitrate and Phosphorus from Agricultural
491 Watersheds in Illinois: Implications for Reducing Nutrient Loading to the Mississippi River, *Environ. Sci. Technol.*, **40**, 4126–
492 4131, <https://doi.org/10.1021/es052573n>, 2006.

493 Runkel, R. L., Crawford, C. G., and Cohn, T. A.: Load Estimator (LOADEST): A FORTRAN program for estimating
494 constituent loads in streams and rivers, <https://doi.org/10.3133/tm4A5>, 2004.

495 Sabo, R. D., Clark, C. M., Gibbs, D. A., Metson, G. S., Todd, M. J., LeDuc, S. D., Greiner, D., Fry, M. M., Polinsky, R., Yang,
496 Q., Tian, H., and Compton, J. E.: Phosphorus Inventory for the Conterminous United States (2002–2012), *J Geophys Res*
497 *Biogeosci.*, **126**, <https://doi.org/10.1029/2020JG005684>, 2021.

498 Sabo, R. D., Pickard, B., Lin, J., Washington, B., Clark, C. M., Compton, J. E., Pennino, M., Bierwagen, B., LeDuc, S. D.,
499 Carleton, J. N., and others: Comparing drivers of spatial variability in US lake and stream phosphorus concentrations, *J.*
500 *Geophys. Res. Biogeosci.*, **128**, e2022JG007227, 2023.

501 Singh, N. K., Van Meter, K. J., and Basu, N. B.: Widespread increases in soluble phosphorus concentrations in streams across
502 the transboundary Great Lakes Basin, *Nature Geoscience* **2023** *16*:10, **16**, 893–900, [https://doi.org/10.1038/s41561-023-
503 *01257-5*, 2023.](https://doi.org/10.1038/s41561-023-01257-5)

504 Skinner, K. D. and Maupin, M. A.: Point-source nutrient loads to streams of the conterminous United States, 2012, Data Series,
505 <https://doi.org/10.3133/DS1101>, 2019.

506 Stackpoole, S. M., Stets, E. G., and Sprague, L. A.: Variable impacts of contemporary versus legacy agricultural phosphorus
507 on US river water quality, *Proc Natl Acad Sci U S A*, **116**, 20562–20567,
508 https://doi.org/10.1073/PNAS.1903226116/SUPPL_FILE/PNAS.1903226116.SAPP.PDF, 2019.

509 Understanding phosphorus: global challenges and solutions: [https://www.unep.org/news-and-stories/story/what-phosphorus-](https://www.unep.org/news-and-stories/story/what-phosphorus-and-why-are-concerns-mounting-about-its-environmental-impact)
510 *and-why-are-concerns-mounting-about-its-environmental-impact*, last access: 26 February 2025.

511 Wang, F., Li, S., Yan, W., Yu, Q., Tian, S., Yan, J., Zhou, D., and Shao, Y.: Dependence of riverine total phosphorus retention
512 and fluxes on hydrology and river size at river network scale, *J. Hydrol. (Amst.)*, **652**, 132676,
513 <https://doi.org/10.1016/j.jhydrol.2025.132676>, 2025a.

514 Wang, Y., Zhang, X., and Zhao, K.: A dataset of riverine nitrogen yield across watersheds in the Conterminous United States,
515 *Scientific Data* **2024** *11*:1, **11**, 1–8, <https://doi.org/10.1038/s41597-024-03552-1>, 2024a.

516 Wang, Y., Zhang, X., Zhao, K., and Singh, D.: Streamflow in the United States: Characteristics, trends, regime shifts, and
517 extremes, *Sci Data*, **11**, 788, <https://doi.org/10.1038/s41597-024-03618-0>, 2024b.

518 Wang, Y., Zhang, X., Zhao, K., Sabo, R. D., Miao, Y., and Clark, C. M.: Riverine Phosphorus Gain and Loss across the
519 conterminous United States, <https://doi.org/10.6084/m9.figshare.28509317>, 2025b.

520 Wilson, D. J.: The harmonic mean *p* -value for combining dependent tests, *Proceedings of the National Academy of Sciences*,
521 **116**, 1195–1200, <https://doi.org/10.1073/pnas.1814092116>, 2019.

522 Withers, P. J. A. and Jarvie, H. P.: Delivery and cycling of phosphorus in rivers: A review, *Science of The Total Environment*,
523 **400**, 379–395, <https://doi.org/10.1016/j.scitotenv.2008.08.002>, 2008.

Deleted: V., David, M. B., and Gentry, L. E.: Timing of riverine export of nitrate and phosphorus from agricultural watersheds in Illinois: Implications for reducing nutrient loading to the Mississippi River, *Environ Sci Technol*, **40**, 4126–4131, <https://doi.org/10.1021/ES052573N/ASSET/IMAGES/LARGE/ES052573NF00004.JPEG>, 2006a.
Royer, T. V., David, M. B., and Gentry, L....

Deleted: ,

Deleted: 2006b

Deleted: ,

Deleted:),

Deleted: 2025

Deleted: extremes

Deleted: 024e

Deleted: Figshare, [data set], <https://doi.org/10.6084/m9.figshare.28509317>, 2025

Formatted: English (UK)

540 Wurtsbaugh, W. A., Paerl, H. W., and Dodds, W. K.: Nutrients, eutrophication and harmful algal blooms along the freshwater
541 to marine continuum, *WIREs Water*, 6, <https://doi.org/10.1002/wat2.1373>, 2019.

542 Xia, Y., Zhang, M., Tsang, D. C. W., Geng, N., Lu, D., Zhu, L., Igalavithana, A. D., Dissanayake, P. D., Rinklebe, J., Yang,
543 X., and Ok, Y. S.: Recent advances in control technologies for non-point source pollution with nitrogen and phosphorous from
544 agricultural runoff: current practices and future prospects, *Appl. Biol. Chem.*, 63, 8, [https://doi.org/10.1186/s13765-020-0493-](https://doi.org/10.1186/s13765-020-0493-6)
545 6, 2020.

546 Zhang, Q. and Hirsch, R. M.: River Water-Quality Concentration and Flux Estimation Can be Improved by Accounting for
547 Serial Correlation Through an Autoregressive Model, *Water Resour. Res.*, 55, 9705–9723,
548 <https://doi.org/10.1029/2019WR025338>, 2019.

549 Zhang, W., Jin, X., Liu, D., Lang, C., and Shan, B.: Temporal and spatial variation of nitrogen and phosphorus and
550 eutrophication assessment for a typical arid river — Fuyang River in northern China, *Journal of Environmental Sciences*, 55,
551 41–48, <https://doi.org/10.1016/J.JES.2016.07.004>, 2017.

Deleted: ,

Deleted: ,

Deleted: ¶